Trap-assisted tunnelling current in MIM structures

Article *in* Open Physics · September 2010

DOI: 10.2478/s11534-010-0027-7

9 authors, including:

Miroslav Mikolášek
Slovak University of Technology in Bratislava
149 PUBLICATIONS **752** CITATIONS
SEE PROFILE

Ralf Granzner
X-FAB Semiconductor Foundries
55 PUBLICATIONS **1,488** CITATIONS
SEE PROFILE

Juraj Breza
Slovak University of Technology, Bratislava, Slovakia
114 PUBLICATIONS **908** CITATIONS
SEE PROFILE

Ladislav Harmatha
Slovak University of Technology in Bratislava
75 PUBLICATIONS **413** CITATIONS
SEE PROFILE

Cent. Eur. J. Phys. • 9(1) • 2011 • 230-241
DOI: 10.2478/s11534-010-0027-7

VERSITA

Central European Journal of **Physics**

Trap-assisted tunnelling current in MIM structures*

Research Article

Juraj Racko[1]**, Miroslav Mikolášek[1], Ralf Granzner[2], Juraj Breza[1], Daniel Donoval[1], Alena Grmanová[1], Ladislav Harmatha[1], Frank Schwierz[2], Karol Fröhlich[3]

1 *Slovak University of Technology, Ilkovičova 3, 812 19 Bratislava, Slovakia*

2 *Technical University of Ilmenau, PF 98684 Ilmenau, Germany*

3 *Slovak Academy of Sciences, Dúbravská cesta 9, 841 04 Bratislava, Slovakia*

Received 9 December 2009; accepted 28 March 2010

Abstract: A new model is presented of current transport in Metal Insulator Metal (MIM) structures by quantum mechanical tunnelling. In addition to direct tunnelling through an insulating layer, tunnelling via defects present in the insulating layer plays an important role. Examples of the influence of the material and thickness of the insulating layer, energy distribution of traps, and metal work functions are also provided.

PACS (2008): 73.40.-c, 73.40.Gk, 73.40.Rw, 73.50.-h, 73.50.Gr

Keywords: MIM • I-V characteristics • trap-assisted tunnelling • high-permittivity dielectrics

1. Introduction

The MIM structure, along with a MOSFET, creates the basic element of the DRAM (Dynamic Random Access Memory). The MIM structure has a high capacitance thanks to the use of a thin dielectric layer with high permittivity, the so-called high-k layer. The structure should be designed to minimize the leakage currents so as to avoid the need to increase the refresh frequency to keep the functionality of the memory element. The leakage current is a consequence of Direct Tunnelling (DT) of free charge carriers through the insulating layer. The current due to DT creates the lower, physically insurmountable limit, which has to be taken into account in the design of the DRAM. In real structures, however, the leakage current reaches a higher value, which stems from tunnelling of charge carriers via a sub-band of deep traps present in the insulator, the so-called traps-assisted tunnelling (TAT) current. The paper presents a new model for calculation and simulation of DT and TAT currents in MIM structures.

2. Theory

Our physical model treats a MIM structure with a thin insulating layer. The energy-band diagram of the struc-

*Presented at the SURFINT–SREN II Conference, November 15-20, 2009, Florence, Italy.

**E-mail: juraj.racko@stuba.sk

ture is shown in Fig. 1. Traditionally, the charge transfer through a thin insulating layer is described by the model of Frenkel-Poole emission [1–3] or by the field-dependent Shockley-Read-Hall (SRG) model modified by Schenk [4] and including tunnelling by Hurkx, [5]. There are many other works dealing with the issue of trap-assisted tunnelling [6, 7] and with thermionic trap-assisted tunnelling in Schottky junctions [8–11]. Our new physical model of TAT considers the fact that the insulating layer contains a high concentration of defects [12]. These defects may be viewed as traps for free charge carriers. The traps lie at energy levels ε and may create a sub-band of traps in the band diagram (see Fig. 1). Their energy distribution within the corresponding sub-band can be described by a Gaussian function

$$D_{\mathrm{t}}^{\mathrm{D,A}}(\varepsilon, x) = \sum_{\mathrm{i}} \frac{N_{\mathrm{t}}^{\mathrm{i\,D,A}}(x)}{E_g\sqrt{2\pi}} \cdot \exp\left(-\left(\frac{\varepsilon - E_{\mathrm{C}}(x) + E_{\mathrm{t}}^{\mathrm{i}}}{2\Delta E_{\mathrm{t}}^{\mathrm{i}}}\right)^2\right), \tag{1}$$

where subscript i denotes the i-th sub-band of traps, E_{g} is the energy band gap, $\Delta E_{\mathrm{t}}^{\mathrm{i}}$ is the width of the i-th sub-band of traps (more exactly, the standard deviation of distribution D_{t}), $E_{\mathrm{t}}^{\mathrm{i}}$ is the distance of the middle of the i-th sub-band of traps from the conduction band edge $E_C(x)$, and $N_{\mathrm{t}}^{\mathrm{i\,D,A}}(x)$ is the concentration of traps in the i-th sub-band of traps. The upper indices denote donor or acceptor traps. The traps are characterized by effective cross-sections for electrons σ^{e} and for holes σ^{h} (m^2).

The model of current transport considers both direct tunnelling (DT) and tunnelling via deep traps present in the insulator (TAT). The resulting current is then given as

$$J_{\mathrm{MIM}} = J_{\mathrm{DT}} + J_{\mathrm{TAT}}. \tag{2}$$

2.1. Direct tunnelling

The current due to DT J_{DT} consists of electron (e) and hole (h) components, and the net current is given by $J_{\mathrm{DT}} = J_{\mathrm{DT}}^{\mathrm{e}} + J_{\mathrm{DT}}^{\mathrm{h}}$. Single current components can be written as [13, 14]

$$J_{\mathrm{DT}}^{\mathrm{e,h}} = A^{*\mathrm{e,h}} T^2 \int_{E_{\mathrm{V}}(x_{\mathrm{M}_2})}^{E_{\mathrm{C}}(x_{\mathrm{M}_1})} \left(\int_{0,-\infty}^{\infty,0} \frac{\Gamma_{\mathrm{DT}}^{\mathrm{e,h}}(E_\perp)\left(\exp\left(\pm\frac{E_{||}+E_\perp-E_{\mathrm{F}_{\mathrm{M}_1}}}{kT}\right) - \exp\left(\pm\frac{E_{||}+E_\perp-E_{\mathrm{F}_{\mathrm{M}_2}}}{kT}\right)\right)}{\left(1+\exp\left(\pm\frac{E_{||}+E_\perp-E_{\mathrm{F}_{\mathrm{M}_1}}}{kT}\right)\right)\left(1+\exp\left(\pm\frac{E_{||}+E_\perp-E_{\mathrm{F}_{\mathrm{M}_2}}}{kT}\right)\right)} dE_{||} \right) dE_\perp, \tag{3}$$

where $A^{*\mathrm{e,h}}$ is the effective Richardson constant of electrons or holes impinging onto the metal-to-insulator potential barrier, $E_{\mathrm{F}_{\mathrm{M}_1}} \equiv 0$ is the reference Fermi level in metal M_1 and $E_{\mathrm{F}_{\mathrm{M}_2}} = -qV_{\mathrm{a}}$ is the Fermi level in metal M_2, where V_{a} is the voltage applied to electrode M_2. The energy of the tunnelling electron or hole has two components, $\varepsilon = E_\perp + E_{||}$. Component $E_\perp$ is the energy perpendicular to the metal-insulator interface (i.e., in the field direction in the insulator), and $E_{||}$ is the energy parallel to the interface. $\Gamma_{\mathrm{DT}}^{\mathrm{e,h}}(E_\perp)$ are transmission coefficients for direct tunnelling of electrons and holes. In the WKB approximation they are calculated as

$$\Gamma_{\mathrm{DT}}^{\mathrm{e,h}}(E_\perp) = \exp\left(-\frac{2}{\hbar}\int_{x_{\mathrm{M}_1}}^{x_{\mathrm{M}_2}} \sqrt{2\, m_{\mathrm{TUN}}^{*\mathrm{e,h}}\,(\pm E_{\mathrm{C,V}}(x) \mp E_\perp)}\, dx\right), \tag{4}$$

where $m_{\mathrm{TUN}}^{*\mathrm{e,h}}$ is the electron or hole tunnelling mass in the field direction.

2.2. Trap-assisted tunnelling

In addition to direct tunnelling through the insulating layer with high permittivity (high-k layer), an important role belongs also to tunnelling via defects present in the insulating layer. The exchange of free carriers between the traps and the metals on the two sides of the MIM structure, and between the traps and the conduction (CB) and valence bands (VB) by thermal generation and recombination, involves twelve processes, shown in Fig. 2.

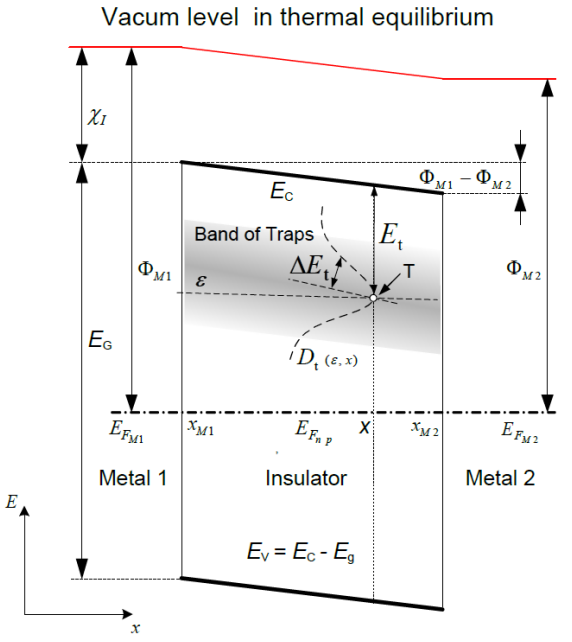

Figure 1. Band diagram of the MIM structure in thermal equilibrium.

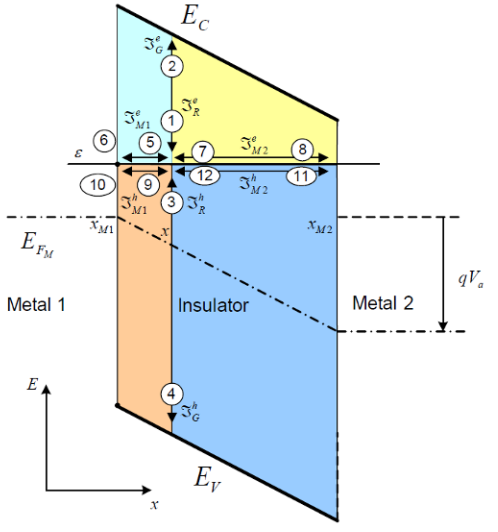

Figure 2. Band diagram for trap-assisted tunnelling (TAT) at applied voltage V_a.

Each of the twelve exchange processes is characterized by its respective charge-carrier transport function $\Im$, defined for both electrons and holes, and describing the rate of free-charge-carrier transport. The charge-carrier transport function divided by elementary charge $\Im/q$ has a dimension of frequency (s^{-1}). Physically, the ratio $q/\Im$ is the period between two subsequent electron (hole) tunnelling processes between the trap and the metal, electron (hole) trapping processes between the CB (VB) and the trap or, finally, electron (hole) emission processes between the trap and the CB (VB).

The charge transport function $\Im$ in our TAT model (belonging to each of the twelve exchange processes) can be expressed comfortably by the following physical quantities: escape times τ, occupation probability of traps by electrons f_t, and the Fermi-Dirac distribution function $f_{M_{1,2}}$, for free electrons in metals M_1 and M_2. Now let us discuss the twelve exchange processes in detail. The following four processes correspond to the classical SRH generation-recombination model.

1. The current of electrons from the conduction band of the insulator trapped by a trap lying in the insulator at place x on energy level ε can be written as

$$\Im^e_R(\varepsilon, x) = q\frac{(1 - f_t(\varepsilon, x))}{\tau^e_R(x)}, \tag{5}$$

with recombination escape time

$$\tau^e_R(x) = (v^e_{th}\sigma^e n(x))^{-1}. \tag{6}$$

The electron concentration in the insulator is given by

$$n(x) = N_C \exp\left(-\frac{E_C(x) - E_{F_n}(x)}{kT}\right), \tag{7}$$

where N_C is the effective CB density of states, and $E_{F_n}(x)$ is the electron quasi-Fermi energy. Function $(1 - f_t(\varepsilon, x))$ in (5) is the probability that the trap centres are not occupied by electrons.

2. The current of electrons emitted from the trap into the conduction band of the insulator is

$$\Im^e_G(\varepsilon, x) = q\frac{f_t(\varepsilon, x)}{\tau^e_G(\varepsilon, x)}, \tag{8}$$

with generation escape time

$$\tau^e_G(\varepsilon, x) = (v^e_{th}\sigma^e n_t(\varepsilon, x))^{-1}, \tag{9}$$

where

$$n_t(\varepsilon, x) = N_C \exp\left(-\frac{E_C(x) - \varepsilon}{kT}\right). \tag{10}$$

3. The hole current from the valence band trapped by the trap is

$$\mathfrak{S}^{\mathrm{h}}_{\mathrm{R}}(\varepsilon, x) = q\frac{f_{\mathrm{t}}(\varepsilon, x)}{\tau^{\mathrm{h}}_{\mathrm{R}}(x)}, \tag{11}$$

with recombination escape time

$$\tau^{\mathrm{h}}_{\mathrm{R}}(x) = \left(v^{\mathrm{h}}_{\mathrm{th}}\sigma^{\mathrm{h}}p(x)\right)^{-1}. \tag{12}$$

The concentration of holes in the insulator is given by

$$p(x) = N_V \exp\left(\frac{E_{\mathrm{V}}(x) - E_{\mathrm{F_p}}(x)}{kT}\right), \tag{13}$$

where N_V is the effective VB density of states and E_{Fp} is the hole quasi-Fermi energy.

4. The current of holes emitted by the trap into the valence band

$$\mathfrak{S}^{\mathrm{h}}_{\mathrm{G}}(\varepsilon, x) = q\frac{(1 - f_{\mathrm{t}}(\varepsilon, x))}{\tau^{\mathrm{h}}_{\mathrm{G}}(\varepsilon, x)}, \tag{14}$$

with generation escape time

$$\tau^{\mathrm{h}}_{\mathrm{G}}(\varepsilon, x) = \left(v^{\mathrm{h}}_{\mathrm{th}}\sigma^{\mathrm{h}}p_{\mathrm{t}}(\varepsilon, x)\right)^{-1}, \tag{15}$$

where

$$p_{\mathrm{t}}(\varepsilon, x) = N_{\mathrm{V}} \exp\left(\frac{E_{\mathrm{V}}(x) - \varepsilon}{kT}\right). \tag{16}$$

These four exchange processes are completed by eight other tunnelling processes assisted by traps.

5. The current of electrons tunnelling from metal $\mathrm{M_1}$ to the trap is

$$\mathfrak{S}^{\mathrm{e}}_{\mathrm{M_1}\to\mathrm{T}}(\varepsilon, x) = q\frac{f_{\mathrm{M_1}}(\varepsilon)\,(1 - f_{\mathrm{t}}(\varepsilon, x))}{\tau^{\mathrm{e}}_{\mathrm{M_1}}(\varepsilon, x)}, \tag{17}$$

where

$$f_{\mathrm{M_1}}(\varepsilon, x_{\mathrm{M_1}}) = \left(1 + \exp\left(\frac{\varepsilon - E_{\mathrm{F}_{\mathrm{M_1}}}(x_{\mathrm{M_1}})}{kT}\right)\right)^{-1} \tag{18}$$

and the tunnelling escape time is

$$\tau^{\mathrm{e}}_{\mathrm{M_1}}(\varepsilon, x) = \frac{q}{A^{*\mathrm{e}}T^2\sigma^{\mathrm{e}}\Pi^{\mathrm{e}}_{\mathrm{M_1}\Leftrightarrow\mathrm{T}}(\varepsilon, x)}. \tag{19}$$

The effective transmission coefficient for trap-assisted tunnelling of electrons $\Pi^{\mathrm{e}}_{\mathrm{M_1}\Leftrightarrow\mathrm{T}}$ is calculated as

$$\Pi^{\mathrm{e}}_{\mathrm{M_1}\Leftrightarrow\mathrm{T}}(\varepsilon, x) = \frac{1}{k^2T^2}\int_{\varepsilon\Rightarrow-\infty}^{\varepsilon}(\varepsilon - E_{\perp})\,\Gamma^{\mathrm{e}}_{\mathrm{M_1}\Leftrightarrow\mathrm{T}}(E_{\perp}, x)\,dE_{\perp}, \tag{20}$$

and the electron transmission coefficient (thus the tunnelling probability of an electron with total energy ε and with energy perpendicular to the metal-insulator interface $E_{\perp}$) $\Gamma^{\mathrm{e}}_{\mathrm{M_1}\Leftrightarrow\mathrm{T}}$ is given, in the WKB approximation, by formula

$$\Gamma^{\mathrm{e}}_{\mathrm{M_1}\Leftrightarrow\mathrm{T}}(E_{\perp}, x) = \exp\left(-\frac{2}{\hbar}\int_{x_{\mathrm{M_1}}}^{x_{\mathrm{T}}}\sqrt{2m^{*\mathrm{e}}_{\mathrm{TUN}}\,(E_{\mathrm{C}}(x) - E_{\perp})}\,dx\right). \tag{21}$$

Except for the integration boundaries, this expression is the same used for calculating the probability of tunnelling in the case of direct tunnelling, Eq. (3).

6. The current of electrons tunnelling from the trap into metal M_1 is

$$\Im^{e}_{T\to M_1}(\varepsilon,x)=q\frac{f_t(\varepsilon,x)\left(1-f_{M_1}(\varepsilon)\right)}{\tau^{e}_{M_1}(\varepsilon,x)}. \tag{22}$$

7. The current of electrons tunnelling from metal M_2 to the trap is

$$\Im^{e}_{M_2\to T}(\varepsilon,x)=q\frac{f_{M_2}(\varepsilon)\left(1-f_t(\varepsilon,x)\right)}{\tau^{e}_{M_2}(\varepsilon,x)}, \tag{23}$$

where

$$f_{M_2}(\varepsilon,x_{M_2})=\left(1+\exp\left(\frac{\varepsilon-E_{F_{M_2}}(x_{M_2})}{kT}\right)\right)^{-1} \tag{24}$$

and the tunnelling escape time is

$$\tau^{e}_{M_2}(\varepsilon,x)=\frac{q}{A^{*e}T^2\sigma^{e}\Pi^{e}_{M_2\Leftrightarrow T}(\varepsilon,x)}, \tag{25}$$

with

$$\Pi^{e}_{M_2\Leftrightarrow T}(\varepsilon,x)=\frac{1}{k^2T^2}\int\limits_{\varepsilon\Rightarrow-\infty}^{\varepsilon}(\varepsilon-E_\perp)\,\Gamma^{e}_{M_2\Leftrightarrow T}(E_\perp,x)\,dE_\perp \tag{26}$$

and

$$\Gamma^{e}_{M_2\Leftrightarrow T}(E_\perp,x)=\exp\left(-\frac{2}{\hbar}\int\limits_{x}^{x_{M_2}}\sqrt{2m^{*e}_{TUN}\left(E_C(x)-E_\perp\right)}\,dx\right). \tag{27}$$

8. The current of electrons tunnelling from the trap into metal M_2 is

$$\Im^{e}_{T\to M_2}(\varepsilon,x)=q\frac{f_t(\varepsilon,x)\left(1-f_{M_2}(\varepsilon)\right)}{\tau^{e}_{M_2}(\varepsilon,x)}. \tag{28}$$

9. The current of holes tunnelling from metal M_1 to the trap is

$$\Im^{h}_{M_1\to T}(\varepsilon,x)=q\frac{f_t(\varepsilon,x)\left(1-f_{M_1}(\varepsilon)\right)}{\tau^{h}_{M_1}(\varepsilon,x)} \tag{29}$$

with tunnelling escape time

$$\tau^{h}_{M_1}(\varepsilon,x)=\frac{q}{A^{*h}T^2\sigma^{h}\Pi^{h}_{M_1\Leftrightarrow T}(\varepsilon,x)}, \tag{30}$$

with

$$\Pi^{h}_{M_1\Leftrightarrow T}(\varepsilon,x)=\frac{1}{k^2T^2}\int\limits_{\varepsilon}^{\varepsilon\Rightarrow\infty}(E_\perp-\varepsilon)\,\Gamma^{h}_{M_1\Leftrightarrow T}(E_\perp,x)\,dE_\perp \tag{31}$$

and

$$\Gamma^{h}_{M_1\Leftrightarrow T}(E_\perp,x)=\exp\left(-\frac{2}{\hbar}\int\limits_{x_{M_1}}^{x}\sqrt{2m^{*h}_{TUN}\left(E_\perp-E_V(x)\right)}\,dx\right). \tag{32}$$

10. The current of holes tunnelling from the trap into metal M_1 is

$$\Im^{h}_{T\to M_1}(\varepsilon,x) = q\frac{f_{M_1}(\varepsilon)\,(1-f_t(\varepsilon,x))}{\tau^{h}_{M_1}(\varepsilon,x)}. \tag{33}$$

11. The current of holes tunnelling from metal M_2 to the trap is

$$\Im^{h}_{M_2\to T}(\varepsilon,x) = q\frac{f_t(\varepsilon,x)\left(1-f_{M_2}(\varepsilon)\right)}{\tau^{h}_{M_2}(\varepsilon,x)}, \tag{34}$$

with tunnelling escape time

$$\tau^{h}_{M_2}(\varepsilon,x) = \frac{q}{A^{*h}T^2\sigma^{h}\Pi^{h}_{M_2\Leftrightarrow T}(\varepsilon,x)}, \tag{35}$$

with

$$\Pi^{h}_{M_2\Leftrightarrow T}(\varepsilon,x) = \frac{1}{k^2T^2}\int_{\varepsilon}^{\varepsilon\Rightarrow\infty}(E_\perp-\varepsilon)\,\Gamma^{h}_{M_2\Leftrightarrow T}(E_\perp,x)\,dE_\perp \tag{36}$$

and

$$\Gamma^{h}_{M_2\Leftrightarrow T}(E_\perp,x) = \exp\left(-\frac{2}{\hbar}\int_{x}^{x_{M_2}}\sqrt{2m^{*h}_{TUN}\,(E_\perp-E_V(x))}\,dx\right). \tag{37}$$

12. The current of holes tunnelling from the trap to metal M_2 is

$$\Im^{h}_{T\to M_2}(\varepsilon,x) = q\frac{f_{M_2}(\varepsilon)\,(1-f_t(\varepsilon,x))}{\tau^{h}_{M_2}(\varepsilon,x)}. \tag{38}$$

The following quantities have been used to define the escape times: $v^{e,h}_{th} = \sqrt{3kT/m^{*e,h}}$ is the thermal electron and hole velocity and $m^{*e,h}$ are effective masses of free electrons in CB or holes in VB.

The twelve exchange processes between the traps, metals M_1 and M_2, and conduction and valence bands must satisfy the balance equation. Under steady-state conditions, the flow of electrons onto the trap must be the same as the rate of electrons released from the trap, which is expressed in the following equation

$$\begin{aligned}&\Im^{e}_{R}-\Im^{e}_{G}+\Im^{h}_{G}-\Im^{h}_{R}+\Im^{e}_{M_1\to T}-\Im^{e}_{T\to M_1}\\&+\Im^{e}_{M_2\to T}-\Im^{e}_{T\to M_2}-\Im^{h}_{M_1\to T}+\Im^{h}_{T\to M_1}\\&-\Im^{h}_{M_2\to T}+\Im^{h}_{T\to M_2}=0.\end{aligned} \tag{39}$$

On inserting respective charge-transport functions for the twelve exchange processes Eqs. (5, 8, 11, 14, 17, 22, 23, 28, 29, 33, 34, and 38) in (39) we obtain

$$\begin{aligned}&\frac{1-f_t(\varepsilon,x)}{\tau^{e}_{R}(x)}-\frac{f_t(\varepsilon,x)}{\tau^{e}_{G}(\varepsilon,x)}-\frac{f_t(\varepsilon,x)}{\tau_{R^h(x)}}+\frac{1-f_t(\varepsilon,x)}{\tau^{h}_{G}(\varepsilon,x)}\\&+\frac{f_{M_1}(\varepsilon)-f_t(\varepsilon,x)}{\tau^{e+h}_{M_1}(\varepsilon,x)}+\frac{f_{M_2}(\varepsilon)-f_t(\varepsilon,x)}{\tau^{e+h}_{M_2}(\varepsilon,x)}=0,\end{aligned} \tag{40}$$

where $\tau^{e+h}_{M_1}$ and $\tau^{e+h}_{M_2}$ are conjoined escape times given by

$$\frac{1}{\tau^{e+h}_{M_1}(\varepsilon,x)} = \left(\frac{1}{\tau^{e}_{M_1}(\varepsilon,x)}+\frac{1}{\tau^{h}_{M_1}(\varepsilon,x)}\right) \tag{41}$$

and

$$\frac{1}{\tau^{e+h}_{M_2}(\varepsilon,x)} = \left(\frac{1}{\tau^{e}_{M_2}(\varepsilon,x)}+\frac{1}{\tau^{h}_{M_2}(\varepsilon,x)}\right). \tag{42}$$

By eliminating $f_t(\varepsilon, x)$ from Eq. (40), we get the probability of trap occupation by an electron

$$f_t(\varepsilon, x) = \tau_{TAT}(\varepsilon, x) \left(\frac{1}{\tau_R^e(x)} + \frac{1}{\tau_G^h(\varepsilon, x)} + \frac{f_{M_1}(\varepsilon)}{\tau_{M_1}^{e+h}(\varepsilon, x)} + \frac{f_{M_2}(\varepsilon)}{\tau_{M_2}^{e+h}(\varepsilon, x)} \right), \tag{43}$$

where

$$\frac{1}{\tau_{TAT}(\varepsilon, x)} = \left(\frac{1}{\tau_R^e(x)} + \frac{1}{\tau_G^e(\varepsilon, x)} + \frac{1}{\tau_R^h(x)} + \frac{1}{\tau_G^h(\varepsilon, x)} + \frac{1}{\tau_{M_1}^{e+h}(\varepsilon, x)} + \frac{1}{\tau_{M_2}^{e+h}(\varepsilon, x)} \right). \tag{44}$$

Now let us treat the trap-assisted tunnelling current J_{TAT} flowing through the MIM structure after applying an external voltage. We can start either by calculating the current flowing between metal M_1 and the traps or the current between metal M_2 and the traps. The current between metal M_1 and the traps is given by the difference of the charge transport functions (17), (22), (29), and (33):

$$\begin{aligned} J_{M_1 \Leftrightarrow T} &= \int_{E_V(x_{M_2})}^{E_C(x_{M_1})} \left\{ \int_{x_{M_1}}^{x_{M_2}} \left(\Im_{M_1 \to T}^e - \Im_{T \to M_1}^e - \Im_{M_1 \to T}^h + \Im_{T \to M_1}^h \right) D_t(\varepsilon, x)\, dx \right\} d\varepsilon = \\ &= q \int_{E_V(x_{M_2})}^{E_C(x_{M_1})} \left\{ \int_{x_{M_1}}^{x_{M_2}} \frac{f_{M_1}(\varepsilon) - f_t(\varepsilon, x)}{\tau_{M_1}^{e+h}(\varepsilon, x)} \tau_{TAT}(\varepsilon, x) D_t(\varepsilon, x)\, dx \right\} d\varepsilon. \end{aligned} \tag{45}$$

The current between metal M_2 and the traps is given as a difference of the charge-transport functions (23), (28), (34), and (38):

$$\begin{aligned} J_{T \Leftrightarrow M_2} &= \int_{E_V(x_{M_2})}^{E_C(x_{M_1})} \left\{ \int_{x_{M_1}}^{x_{M_2}} \left(\Im_{M_2 \to T}^e - \Im_{T \to M_2}^e - \Im_{M_2 \to T}^h + \Im_{T \to M_2}^h \right) D_t(\varepsilon, x)\, dx \right\} d\varepsilon = \\ &= q \int_{E_V(x_{M_2})}^{E_C(x_{M_1})} \left\{ \int_{x_{M_1}}^{x_{M_2}} \frac{f_{M_2}(\varepsilon) - f_t(\varepsilon, x)}{\tau_{M_2}^{e+h}(\varepsilon, x)} \tau_{TAT}(\varepsilon, x) D_t(\varepsilon, x)\, dx \right\} d\varepsilon. \end{aligned} \tag{46}$$

On inserting Eq. (43) for f_t we get

$$J_{M_1 \Leftrightarrow T} = \int_{E_C(x_{M_2})}^{E_C(x_{M_1})} \left\{ \int_{x_{M_1}}^{x_{M_2}} \left(\frac{f_{M_1} - f_{M_2}}{\tau_{M_2}^{e+h} \tau_{M_1}^{e+h}} - \left(\frac{1 - f_{M_1}}{\tau_R^e \tau_{M_1}^{e+h}} - \frac{f_{M_1}}{\tau_G^e \tau_{M_1}^{e+h}} - \frac{f_{M_1}}{\tau_R^h \tau_{M_1}^{e+h}} + \frac{1 - f_{M_1}}{\tau_G^h \tau_{M_1}^{e+h}} \right) \right) \tau_{TAT} D_t\, dx \right\} d\varepsilon, \tag{47}$$

$$J_{T \Leftrightarrow M_1} = \int_{E_C(x_{M_2})}^{E_C(x_{M_1})} \left\{ \int_{x_{M_1}}^{x_{M_2}} \left(\frac{f_{M_2} - f_{M_1}}{\tau_{M_1}^{e+h} \tau_{M_2}^{e+h}} - \left(\frac{1 - f_{M_2}}{\tau_R^e \tau_{M_2}^{e+h}} - \frac{f_{M_2}}{\tau_G^e \tau_{M_2}^{e+h}} - \frac{f_{M_2}}{\tau_R^h \tau_{M_2}^{e+h}} + \frac{1 - f_{M_2}}{\tau_G^h \tau_{M_2}^{e+h}} \right) \right) \tau_{TAT} D_t\, dx \right\} d\varepsilon. \tag{48}$$

Let us assume that the insulating layer

- is "sufficiently" thin so that tunnelling between the traps and metallic electrodes is intensive, and
- the traps in the energy band gap are located at deep levels: $(E_C - E_t) \geqslant 0.5$ eV.

In this case, the first term $\left(f_{M_1} - f_{M_2}\right) / \left(\tau_{M_2}^{e+h} \tau_{M_1}^{e+h}\right)$ in equations (47) and (48) dominates. This term represents

the difference between the currents of electrons and holes tunnelling from metal M_1 into metal M_2 via the traps $\left(M_1 \overset{e+h}{\Leftrightarrow} T \overset{e+h}{\Leftrightarrow} M_2\right)$. The remaining four terms in Eqs. (47) and (48), in denominators containing both the tunnelling escape times and recombination and generation escape times, contribute little to the overall current. In our simulations (see below), the contribution of these terms was lower by 4 to 6 orders of magnitude than the contribution of the dominating term. The reason is that under steady-state conditions, the concentration of free electrons and holes in the insulator is virtually zero: $n(x) \approx 0$ in Eq. (7) and $p(x) \approx 0$ in Eq. (13). (We do not assume the presence of shallow donor or acceptor levels.) The recombination escape times are then $\tau_R^e(x) \approx \infty$ in Eq. (6) and $\tau_R^h(x) \approx \infty$ in Eq. (12). Similarly the generation escape times (Eqs. (9) and (15)) are much larger than the tunnelling escape times: $\tau_G^{e,h}(x) \gg \tau_{M_1}^{e+h}, \tau_{M_2}^{e+h}$. This is because the concentrations of electrons n_t in Eq. (10) and holes p_t in Eq. (16) are very low if the traps are located deep in the energy-band gap of the insulator. This is why all recombination and generation terms in expressions (40), (43), and (44), in which the escape times τ_R^e, τ_R^h, τ_G^e, and τ_G^h occur in the denominator, can be neglected.

Physical interpretation of the less important terms in Eq. (47) follows:

- Term $\left(1 - f_{M_1}\right) / \left(\tau_R^e \tau_{M_1}^{e+h}\right)$ describes the flow of electrons trapped by the traps from CB, and tunnelling further into metal M_1 $\left(CB \overset{e}{\to} T \overset{e}{\to} M_1\right)$;
- Term $f_{M_1} / \left(\tau_G^e \tau_{M_1}^{e+h}\right)$ describes the flow of electrons tunnelling from metal M_1 onto the traps and then being emitted into the conduction band CB $\left(M_1 \overset{e}{\to} T \overset{e}{\to} CB\right)$;
- Term $f_{M_1} / \left(\tau_R^h \tau_{M_1}^{e+h}\right)$ describes the flow of holes trapped by the traps from the valence band and then tunnelling to metal M_1 $\left(VB \overset{h}{\to} T \overset{h}{\to} M_1\right)$,
- Term $\left(1 - f_{M_1}\right) / \left(\tau_G^h \tau_{M_1}^{e+h}\right)$ describes the flow of holes tunnelling from metal M_1 on the traps and then being emitted into the valence band $\left(M_1 \overset{h}{\to} T \overset{h}{\to} VB\right)$.

The terms in Eq. (48) can be interpreted in a similar way; one simply has to replace metal M_1 by metal M_2. If the absolute values in Eq. (47) satisfy

$$\left|\frac{f_{M_1} - f_{M_2}}{\tau_{M_2}^{e+h} \tau_{M_1}^{e+h}}\right| \gg \left|\frac{1 - f_{M_1}}{\tau_R^e \tau_{M_1}^{e+h}} - \frac{f_{M_1}}{\tau_G^e \tau_{M_1}^{e+h}} - \frac{f_{M_1}}{\tau_R^h \tau_{M_1}^{e+h}} + \frac{1 - f_{M_1}}{\tau_G^h \tau_{M_1}^{e+h}}\right|, \tag{49}$$

and in Eq. (48) it holds that

$$\left|\frac{f_{M_2} - f_{M_1}}{\tau_{M_1}^{e+h} \tau_{M_2}^{e+h}}\right| \gg \left|\frac{1 - f_{M_2}}{\tau_R^e \tau_{M_2}^{e+h}} - \frac{f_{M_2}}{\tau_G^e \tau_{M_2}^{e+h}} - \frac{f_{M_2}}{\tau_R^h \tau_{M_2}^{e+h}} + \frac{1 - f_{M_2}}{\tau_G^h \tau_{M_2}^{e+h}}\right|, \tag{50}$$

then the currents in Eqs. (47) and (48) are reduced so that $J_{M_1 \Leftrightarrow T} \approx -J_{T \Leftrightarrow M_2}$, and the net current J_{TAT} due to trap-assisted tunnelling in the MIM structure is expressed as

$$J_{TAT} \cong J_{M_1 \Leftrightarrow T} \approx -J_{T \Leftrightarrow M_2} = q \int_{E_V(x_{M_2})}^{E_C(x_{M_1})} \left(\int_{x_{M_1}}^{x_{M_2}} \frac{f_{M_1}(\varepsilon) - f_{M_2}(\varepsilon)}{\tau_{M_1}^{e+h}(\varepsilon, x) + \tau_{M_2}^{e+h}(\varepsilon, x)} D_t(\varepsilon, x)\, dx \right) d\varepsilon. \tag{51}$$

Here we utilize the fact that the escape time τ_{TAT} defined by Eq. (44) reduces to $1/\tau_{TAT} \cong \left(1/\tau_{M_1}^{e+h} + 1/\tau_{M_2}^{e+h}\right)$ by neglecting the recombination and generation term. In principle it means that we neglect the four exchange processes representing the classical Shockley-Read-Hall model of generation and recombination.

For evaluating E_C and E_V it is enough to solve the Poisson equation:

$$-\frac{d}{dx}\left(\kappa \frac{d\psi}{dx}\right) \cong \frac{q}{\varepsilon_0}\left\{\int_{E_V}^{E_C} D_t^D\,(1 - f_t)\, d\varepsilon - \int_{E_V}^{E_C} D_t^A f_t\, d\varepsilon\right\}. \tag{52}$$

Assuming that the right side of the Poisson equation contains only very small values, the field intensity in the whole bulk of the insulator is constant, and for approximate values of $E_C(x)$ and $E_{F_{n,p}}(x)$ we get

$$E_C(x) \cong \Phi_{M_1} - \chi_I - \frac{x - x_{M_1}}{x_{M_2} - x_{M_1}}\left(\Phi_{M_1} - \Phi_{M_2} - q V_a\right), \tag{53}$$

$$E_{F_{n,p}}(x) \cong q \frac{x - x_{M_1}}{x_{M_2} - x_{M_1}} V_a, \tag{54}$$

where Φ_{M_1} and Φ_{M_2} are the work functions of metals M_1 and M_2, χ_I is the electron affinity of the insulation layer, and V_a is the external voltage.

3. Results

In the first simulation we show how the energy distribution of traps in the insulator $D_t(\varepsilon, x)$ affects the net

current flowing through the structure on applying an external voltage V_a. The parameters of the sub-band of traps (1) are varied by means of three variables: N_t, E_t, and ΔE_t. In our simulations only one sub-band of acceptor or donor traps is considered, where the maximum value N_t of the Gaussian distribution of traps concentration within the sub-band is constant. For $I-V$ simulations this type of defect does not play a role. The simulations demonstrate how these parameters change the shape of the $I-V$ curves of the MIM structure. We have chosen a MIM structure with a 4 nm thick TiO_2 layer (with κ=120) having an energy band gap E_g=3.5 eV, electron affinity χ_I=3.9 eV, and metallic contacts with work functions $\Phi_{M_1} = \Phi_{M_2}$=5.0 eV. Further, the following material parameters have been chosen: trapping cross-sections for electrons and holes $\sigma^e = \sigma^h = 5 \times 10^{-20}$ m^2; the effective Richardson constant for electrons and holes in dielectric layer $A^{*e,h} = 1.0\,A$, where the Richardson constant for free electrons is $A = \left(4\pi q m_0 k^2\right)/h^3$; effective tunnelling electron and hole masses $m^{*e,h}_{TUN} = 0.3\ m_0$; and the effective mass of free electrons in CB or holes in VB is $m^{*e,h} = 0.3\ m_0$.

The net current J_{MIM} flowing through the MIM structure contains contributions from direct tunnelling J_{DT} and from trap-assisted tunnelling J_{TAT}. This contribution depends on the distribution of traps $D_t(\varepsilon, x)$. Figure 3 shows the contributions of J_{DT} and J_{TAT} dependent on the overall density of traps N_T. The density of traps is given by

$$N_T(x) = \int_{E_V}^{E_C} D_t^{D,A}(\varepsilon, x)\, d\varepsilon. \qquad (55)$$

The density of traps has been varied by changing the maximum trap concentration in the middle of the sub-band of traps: N_t=10^{21}, 10^{22}, 10^{23}, 10^{24}, and 10^{25} m^{-3}. The middle of the band of traps E_t was located 1 eV below the conduction band E_C in the forbidden band of the insulator. The width of the sub-band of traps was kept constant, ΔE_t=0.075 eV. Having chosen the parameters in this way, the overall density of traps in the insulator was N_T=3×10^{19}, 3×10^{20}, 3×10^{21}, 3×10^{22}, and 3×10^{23} m^{-3}. As can be seen in Fig. 3, at small voltages the net current J_{MIM} is dominated by trap-assisted tunnelling, while at larger voltages direct tunnelling dominates. The transition between the two regions strongly depends on the trap density, since N_t basically acts as a prefactor to J_{TAT}.

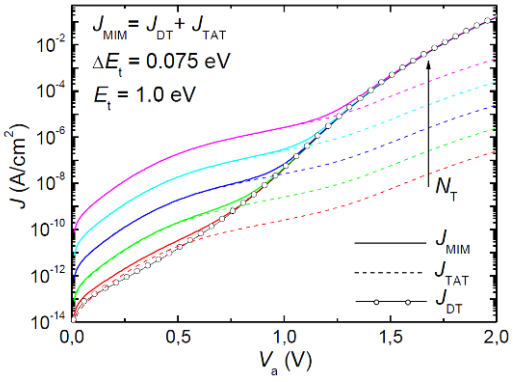

Figure 3. $I-V$ curves (solid lines) of a MIM structure with a 4 nm thick TiO_2 layer with various overall trap densities, N_T=3×10^{19}, 3×10^{20}, 3×10^{21}, 3×10^{22}, and 3×10^{23} m^{-3}. The middle of the sub-band of traps E_t is located 1 eV below the conduction band, and the width of the sub-band is ΔE_t = 0.075 eV. Dashed lines denote the contributions of trap-assisted tunnelling, while the solid line with symbols denotes the direct tunnelling current.

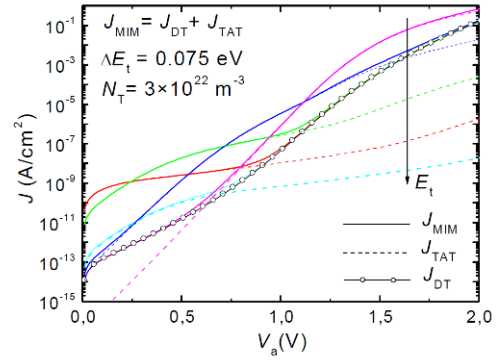

Figure 4. $I-V$ curves of a MIM structure with a 4 nm thick TiO_2 layer, with varying positions of the middle of the sub-band of traps: 0.5, 0.75, 1.0, 1.25, and 1.5 eV below the conduction band in the energy-band gap of the insulator. The overall density of traps was set to N_T=3×10^{22} m^{-3}, and the width of the sub-band was ΔE_t = 0.075 eV.

Figure 4 shows the contributions of direct J_{DT} and trap-assisted tunnelling J_{TAT}, dependent on the position of the middle of the sub-band of traps in the energy-band gap of the insulator. This position is expressed through E_t, the conduction band edge E_C considered as a reference. Simulations demonstrate a strong effect of E_t upon the total current. If E_t lies close to the intrinsic level (middle of the sub-band gap), then trap-assisted tunnelling prevails at low applied voltages. As E_t shifts towards the conduction band, the voltage dependence of J_{TAT} changes.

For E_t <0.75 eV, J_{TAT} becomes smaller than J_{DT} at small voltages and eventually at E_t=0.5 eV the situation is completely different, compared to larger E_t. Now, direct tunnelling dominates at low V_a, while trap-assisted tunnelling prevails at large V_a.

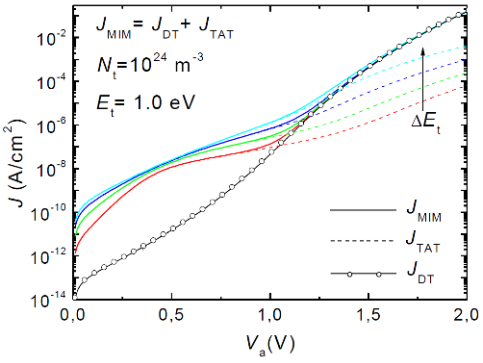

Figure 5. $I-V$ curve of a MIM structure with a 4 nm thick TiO_2 layer with various widths of the sub-band of traps ΔE_t=0.025, 0.05, 0.075, and 0.1 eV.

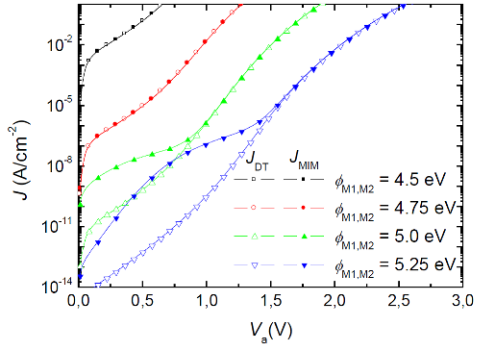

Figure 6. $I-V$ curve of a MIM structure with a 4 nm thick TiO_2 layer. The parameters of sub-band of traps: $N_t = 10^{24}$ m^{-3}, $E_t = 1.0$ eV, and $\Delta E_t = 0.075$ eV. The work functions are $\Phi_{M_1} = \Phi_{M_2} = 4.5, 4.75, 5.0$, and 5.25 eV.

Figure 5 shows the contributions of J_{DT} and J_{TAT} to the net current J_{MIM}, dependent on the width of the sub-band of traps characterized by ΔE_t. The values of the two remaining parameters were kept constant: E_t=1.0 eV and N_t=10^{24} m^{-3}. As it is expected, with the increase of ΔE_t the calculated tunnelling current also increases. Figure 5 shows that the narrower the sub-band of traps, the more pronounced the "hump" in the lower part of the $I-V$ curve. Parameters of the sub-band of traps only affect J_{TAT}, not the direct tunnelling current J_{DT}. The choice of the metallic electrodes, however, affects both of these components.

This is illustrated in Fig. 6, presenting simulations of the $I-V$ curve of a MIM structure with identical metallic electrodes and variations of work functions $\Phi_{M_1} = \Phi_{M_2}$ =4.5, 4.75, 5.0, and 5.25 eV. Simulations reveal how strongly the leakage current depends on the choice of the electrode material.

Direct tunnelling is related to the barrier, defined as a difference between the work function of the metal and the affinity of the insulating layer. For metals with a low work function, the direct tunnelling current J_{DT} dominates along the whole $I-V$ curve. In the case of higher work functions, the contribution of J_{DT} to the overall leakage current becomes less significant, and trap-assisted tunnelling starts to be of major importance ($J_{MIM} \approx J_{TAT}$ for low voltages). However, for the range of work functions considered, it is generally valid that the higher the work function, the smaller the leakage currents. For larger work functions, however, hole tunnelling might become dominant and the net current would increase again. Respective contributions depend strongly on the distribution of traps D_t.

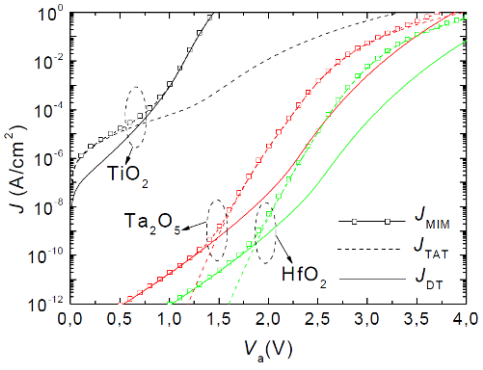

Figure 7. $I-V$ curves of MIM structures for different types of high-κ materials with a 3 nm thick isolating layer. Parameters of the sub-band of traps: N_t=10^{24} m^{-3} (equal to the overall density of traps N_t=3×10^{22} m^{-3}), E_t = 0.75 eV, and ΔE_t = 0.075 eV. The metal work functions are $\Phi_{M_1} = \Phi_{M_2} = 5.0$ eV.

material	E_G (eV)	χ_I (eV)	Φ_{Mid} (eV)	κ (-)
TiO_2	3.5	3.9	5.65	120
Ta_2O_5	4.5	2.8	5.05	20
HfO_2	5.7	2.55	5.4	18

Table 1. Parameters of insulating materials used in simulations.

The effect of the dielectric layer upon the leakage current is even stronger than that of the metallic electrodes. This is shown in Fig. 7, which displays $I-V$ characteristics of MIM structures with 3 nm thick dielectric layers of different high-k materials (TiO_2, Ta_2O_5, and HfO_2). The parameters of these dielectric materials are summarized in Table 3 [15]. The work function Φ_{Mid} represents the ideal value calculated as $\Phi_{Mid} = \chi_I + \frac{E_G}{2}$ (assuming $m^{*e}_{TUN} = m^{*h}_{TUN}$), for which the direct tunnelling current has the lowest magnitude. The highest leakage current has been observed in the structure with TiO_2, which, however, has the highest relative permittivity ($\kappa = 120$) among the insulators studied.

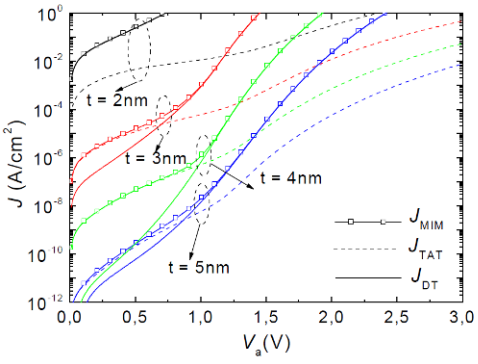

Figure 8. $I-V$ curves of MIM structures with variously thick TiO_2 layers, t=2, 3, 4, and 5 nm. The parameters of the sub-band of traps are N_t=10^{24} m^{-3}, E_t=1.0 eV, and ΔE_t=0.075 eV. The work functions are $\Phi_{M_1} = \Phi_{M_2} = 5.0$ eV.

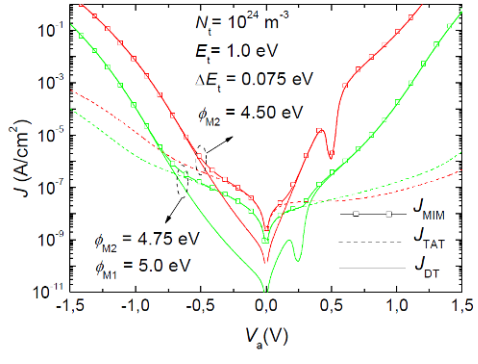

Figure 9. $I-V$ curve of a MIM structure with a 4 nm thick TiO_2 layer with a work function of the second metal electrode Φ_{M_2}=5.0 eV, and two different values of work functions for the first metal electrode: $\Phi_{M_1} = 4.50$ eV, 4.75 eV.

The leakage current might be reduced by increasing the thickness of the insulating layer. This is shown in Fig. 8. As the thickness of the insulator is increased, both components J_{TAT} and J_{DT} are reduced. The strongest relative contribution of trap-assisted tunnelling to the net current can be seen at a thickness of about 4 nm.

Figure 9 shows how the $I-V$ curves of the MIM structure differ on changing the polarity of the applied voltage, in case we use metallic electrodes with different work functions. The higher the difference in the work functions of the two electrodes, the more marked the asymmetry of the $I-V$ curves. The negative differential resistance observed (local minimum in the direct tunnelling current J_{DT}) is because in this region, the tunnelling probability of free carriers $\Gamma^{e,h}_{DT}$ falls faster with applied voltage V_a than the exponential growth of the terms in Eq. (3) containing Fermi-Dirac distribution functions. Obviously, the shift of the local minimum in the $I-V$ characteristics corresponds to the difference of the work functions between the two metal electrodes.

4. Conclusion

This model and simulation of the leakage currents in MIM structures allow the prediction and physical interpretation of the experimental characteristics. By comparing the simulated results with those achieved experimentally, one can analyze the defects present in dielectric layers. After some modification, the model can also be applied to Schottky structures. However, unlike in a MIM structure, in a doped Schottky structure one cannot neglect the generation-recombination processes. In this case one can exactly solve the continuity equations for electrons and holes, incorporating the generation-recombination rates and additional tunnelling rates of the exchange processes between the trap and conduction or valence band. We believe that such a modified TAT model can explain the origin of high gate currents in MIM structures, with small modifications in A_3B_5 compound semiconductor devices with broad energy-band gaps and naturally high concentrations of traps (e.g., AlGaN/GaN HEMTs).

5. Acknowledgement

The work has been conducted in the Centre of Excellence CENAMOST (Slovak Research and Development Agency Contract No. VVCE-0049-07), supported by projects APVV-20-0554-05 and APVV-0133-07 and projects VEGA 1/0742/08, VEGA 1/0507/09 and VEGA 1/0601/10.

References

[1] J. Frenkel, Phys. Rev. 54, 647 (1938)
[2] S.M. Sze, J. Appl. Phys. 38, 2951 (1967)
[3] S.M. Sze, Physics of Semiconductors Devices, second edition (John Wiley & Sons, New York, 1981)
[4] A. Schenk, Solid State Electron. 35, 1585 (1992)
[5] G.A.M. Hurkx, D.B.M. Klaassen, M.P.G. Knuvers, IEEE T. Electron Dev. 39, 331 (1992)
[6] B. Eitan, A. Kolodny, Appl. Phys. Lett. 43, 106 (1983)
[7] D. Ielmini, A.S. Spinelli, A.L. Lacaita, A. Martinelli, G. Ghidini, Solid State Electron. 45, 1361 (2001)
[8] D.M. Sathaiya, S. Karmalkar, IEEE T. Electron Dev. 55, 557 (2008)
[9] D.M. Sathaiya, S. Karmalkar, J. Appl. Phys. 99, 093701 (2006)
[10] S. Karmalkar, D.M. Sathaiya, Appl. Phys. Lett. 82, 3976 (2003)
[11] S. Karmalkar, N. Satyan, D.M. Sathaiya, IEEE Electr. Device L. 27, 87 (2006)
[12] J. Racko et al., In: J. Prášek, M. Adámek, I. Szendiuch (Eds.), 32nd International Spring Seminar on Electronics Technology, 13-17 May 2009, Brno, Czech Republic (Brno University of Technology, Brno, 2009) 256
[13] J. Racko et al., Solid State Electron. 52, 1755 (2008)
[14] J. Racko et al., J. Electr. Eng. 59, 81 (2008)
[15] K. Fröhlich et al., J. Vac. Sci. Technol. B 27, 266 (2009)